



Kinetic studies on the reaction of cob(II)alamin with hypochlorous acid: Evidence for one electron oxidation of the metal center and corrin ring destruction

Rohan S. Dassanayake^{a,1}, Mohamed M. Farhath^a, Jacob T. Shelley^a, Soumitra Basu^a, Nicola E. Brasch^{b,*}

^a Department of Chemistry and Biochemistry, Kent State University, Kent, OH 44242, USA

^b School of Applied Sciences, Auckland University of Technology, Private Bag 92006, Auckland 1142, New Zealand

ARTICLE INFO

Article history:

Received 14 October 2015

Received in revised form 7 July 2016

Accepted 13 July 2016

Available online 15 July 2016

Keywords:

Vitamin B₁₂

Cobalamins

Hypochlorous acid, kinetics

Corrin ring destruction

ABSTRACT

Kinetic and mechanistic studies on the reaction of a major intracellular vitamin B₁₂ form, cob(II)alamin (Cbl(II)), with hypochlorous acid/hypochlorite (HOCl/OCl⁻) have been carried out. Cbl(II) (Co(II)) is rapidly oxidized by HOCl to predominately aquacobalamin/hydroxycobalamin (Cbl(III), Co(III)) with a second-order rate constant of $2.4 \times 10^7 \text{ M}^{-1} \text{ s}^{-1}$ (25.0 °C). The stoichiometry of the reaction is 1:1. UHPLC/HRMS analysis of the product mixture of the reaction of Cbl(II) with 0.9 mol equiv. HOCl provides support for HOCl being initially reduced to Cl• and subsequent H atom abstraction from the corrin macrocycle occurring, resulting in small amounts of corrinoid species with two or four H atoms fewer than the parent cobalamin. Upon the addition of excess (H)OCl further slower reactions are observed. Finally, SDS-PAGE experiments show that HOCl-induced damage to bovine serum albumin does not occur in the presence of Cbl(II), providing support for Cbl(II) being an efficient HOCl trapping agent.

© 2016 Elsevier Inc. All rights reserved.

1. Introduction

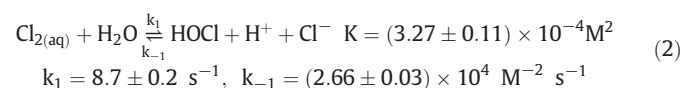
Hypochlorous acid (HOCl) is a potent oxidant secreted by neutrophils and monocytes that is generated via the myeloperoxidase (MPO) catalyzed reaction of chloride with hydrogen peroxide, Eq. (1) [1].



HOCl plays a key role in the innate immune system response against pathogens and microbes, reacting with superoxide to generate •OH [1, 2]. Under inflammatory conditions, production of HOCl by neutrophils reaches ~5 mM [3,4]. High levels of (H)OCl have been linked to multiple diseases including cancer, atherosclerosis and diabetic complications [1, 5]. The involvement of MPO-derived HOCl in neurodegenerative diseases including Parkinson's disease and Alzheimer's disease is also well known [1,6]. (H)OCl undergoes numerous reactions with biomolecules, including chlorination of amines and unsaturated lipids, oxidative bleaching of heme groups and iron sulfur cluster proteins, oxidation of thiols and oxidation of nucleic acids [1,7–17]. Several sensitive intracellular detection methods have recently been developed for detecting (H)OCl using luminescent probes [18,19]. The reactions of (H)OCl

with a variety of transition metal complexes have been reported. Transition metal ions such as Ir(IV), Cu(II) and Ni(II) can catalyze the decomposition of (H)OCl [20]. Several kinetic studies report the oxidation of transition metal complexes by (H)OCl, including coordination complexes of Mn(III) [21], Ni(II) [22], U(IV) [23], V(III) [24], Pt(II) [25], Fe(II) [26], Co(III) [3] and Cr(III) [27].

In the presence of chloride, HOCl is in equilibrium with chlorine under acidic conditions, Eq. (2) [25]. Cl₂ is also a potent oxidizing and chlorinating agent, and indeed, it has recently been proposed that Cl₂, not (H)OCl, is the oxidizing and chlorinating agent generated by the myeloperoxidase/H₂O₂/Cl⁻ system [8,28]. Cl₂ is a strong 2e⁻ oxidant and a weaker 1e⁻ oxidant ($E^\circ \text{Cl}_2/2\text{Cl}^- = 1.36 \text{ V}$ versus NHE at pH 5.0; $E^\circ \text{Cl}_2/\text{Cl}_2^- = 0.43 \text{ V}$ versus NHE at pH 5.0) [22].



Vitamin B₁₂ and its derivatives, also known as cobalamins (Cbls), are essential coenzymes in living organisms. The two mammalian B₁₂-dependent enzyme reactions require either one of the cob(III)alamin (Co³⁺) cofactors adenosylcobalamin (AdoCbl, X = 5'-deoxy-5'-adenosyl (Ado), Fig. 1) or methylcobalamin (MeCbl, X = CH₃, Fig. 1) [29,30]. Methylmalonyl-coenzyme A mutase (MM-CoA mutase) utilizes AdoCbl as a cofactor to catalyze a carbon skeleton rearrangement resulting in the conversion of R-methylmalonyl-CoA to succinyl-CoA,

* Corresponding author.

E-mail address: nbrasch@aut.ac.nz (N.E. Brasch).

¹ Current address: Fiber and Biopolymer Research Institute, Department of Plant and Soil Science, Texas Tech University, Lubbock, TX, 79403, USA.

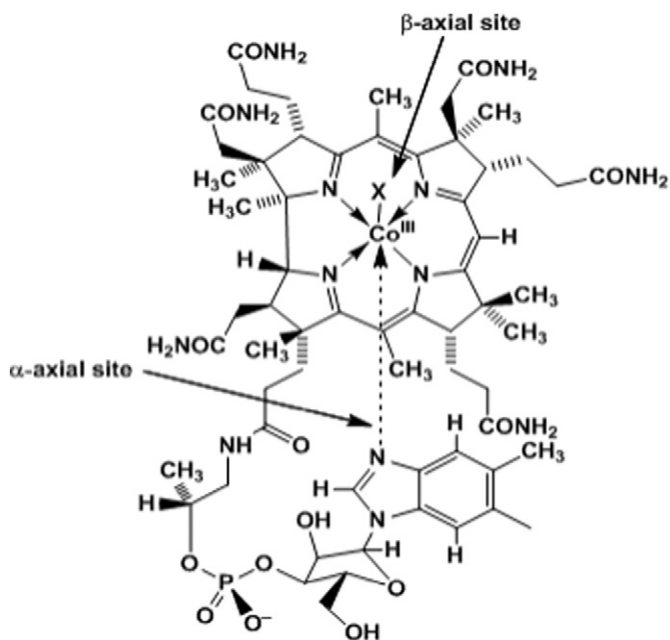


Fig. 1. The structure of cob(III)alamin. X = CN⁻, CH₃, Ado, H₂O, etc.

an important step in the extraction of energy from several amino acids and odd chain fatty acids. Methylcobalamin-dependent methionine synthase catalyzes the methylation of homocysteine (Hcy) to methionine (Met) by 5-methyltetrahydrofolate. Pentacoordinate cob(II)alamin (Cbl(II), Co²⁺) is also an important intracellular Cbl derivative. Cob(III)alamin is reduced to Cbl(II) in a reaction catalyzed by the reductase CblC upon cellular uptake [31]. With B₁₂ supplementation intracellular amounts of both protein-bound and free (non-protein bound) B₁₂ are significant [32–36].

Studies on the reactions of vitamin B₁₂ derivatives with reactive oxygen species (ROS) are of interest for a number of reasons. Cell studies have shown that for at least some ROS, B₁₂ supplementation reduces ROS-induced intracellular oxidative stress [37–39]. In addition, a significant fraction of B₁₂ bound to the B₁₂ transport proteins in the circulation, transcobalamin and haptocorrin, are “Cbl analogs”; that is, corrinoid complexes incapable of serving as cofactors for B₁₂-dependent enzyme reactions [40]. Furthermore patients with neurological diseases and the elderly have higher plasma levels of Cbl analogs [41,42]. Elevated ROS levels are associated with neurological disorders and aging in general. It has been proposed that some of the Cbl analogs result from endogenous modifications of the Cbl corrin ring by oxidants [43]. It is, therefore, of interest to study the reactivity of ROS with B₁₂ derivatives, in part to establish which ROS simply oxidize the metal center of reduced cobalamins versus those that degrade the corrin ring to produce an analog of B₁₂. In this study we present studies on the kinetics and mechanism of the reaction of cob(II)alamin, a major intracellular of B₁₂, with hypochlorous acid. In addition to rapid oxidation of the metal center of Cbl(II), evidence was found for decomposition of the corrin ring by (H)OCl.

2. Experimental section

2.1. Chemicals

Hydroxycobalamin hydrochloride, HOcbl·HCl (·nH₂O) (≥96%, 10–15% water, batch dependent [44]) was purchased from Fluka. Sodium borohydride (≥98%), silver nitrate, and acetic acid were obtained from Acros Organics. Potassium dihydrogen phosphate, sodium hydroxide, ammonia, acetonitrile (HPLC grade), methanol (LC-MS grade), water (HPLC grade), potassium cyanide (≥99%) and sodium hypochlorite

(12–13% by w/w) were purchased from Fisher Scientific. Bovine serum albumin was purchased from Bio-Rad. Water was purified using a Barnstead Nanopure Diamond water purification system.

2.2. Preparation of anaerobic solutions and kinetic measurements

Solutions prepared for Cbl(II) work were degassed by bubbling through argon for at least 2 h. (H)OCl solutions were freshly prepared. It has been shown that buffers (phosphate, carbonate, borate, acetate) have little effect on the rate of decomposition of (H)OCl [45]. Preparation of all anaerobic solutions were carried out in an MBRAUN Labmaster 130 (1250/78) glove box filled with argon, equipped with O₂ and H₂O sensors and a freezer at –24 °C. Air-free UV–Vis spectrometric measurements were carried out in Schlenk cuvettes (cuvettes fitted with a J-Young or an equivalent stopcock) using a Cary 5000 spectrophotometer equipped with a thermostated (25.0 ± 0.1 °C) cell changer operating with WinUV Bio software (version 3.00). Kinetic data for rapid reactions were collected under strictly anaerobic conditions at 25.0 ± 0.1 °C using an Applied Photophysics SX20 stopped-flow spectrophotometer equipped with a photodiode array detector in addition to a single wavelength detector, with sequential mixing capabilities. A continuous flow of nitrogen was used to maintain anaerobic conditions. Data was collected with Pro-Data SX (version 2.1.4) and Pro-Data Viewer (version 4.1.10) software, and a 1.0 or 0.2 cm pathlength cell was utilized. All data was analyzed using Microcal Origin version 8.0.

2.3. pH measurements

pH measurements were carried out at room temperature using an Orion model 710A pH meter equipped with Mettler-Toledo Inlab 421 or 423 pH electrodes. The electrode was filled with a 3 M KCl/saturated AgCl solution (pH 7.00) and standardized with standard buffer solutions at pH 8.60–12.00. Solution pH was adjusted using H₃PO₄, NaOH, or KOH solutions as necessary. The error in the pH values is estimated to be ±0.04.

2.4. Synthesis of cob(II)alamin (Cbl(II))

Cbl(II) was synthesized using a previously described procedure [38].

2.4.1. Determination of cobalamin (Cbl) concentrations

Cbl concentrations were determined by converting Cbls to dicyanocobalamin, (CN)₂Cbl⁻, by reacting with KCN (0.10 M, pH 11.50). The concentration of the final product was determined using UV–Vis spectrometry ($\epsilon_{368 \text{ nm}} = 30 \text{ mM}^{-1} \text{ cm}^{-1}$) [46].

2.5. Synthesis of chloride-free sodium hypochlorite

Anaerobic solutions of sodium hypochlorite were freshly prepared to minimize the disproportionation of hypochlorite [47]. Commercially available NaOCl contains ~10% (w/w) chloride. Chloride-free NaOCl was prepared by extraction with ethyl acetate [8]. NaOCl (100 ml) mixed with ethyl acetate (100 ml) was protonated by drop wise addition of phosphoric acid (final pH of the solution was 6.00) with intermittent shaking. The organic phase containing HOCl was washed three times with H₂O, and HOCl was re-extracted into the aqueous phase by the drop wise addition of NaOH (final pH of the solution was 9.00). The residual ethyl acetate in the aqueous phase was removed by vigorous bubbling with N₂ gas [8]. The final concentrations of both commercially available NaOCl and chloride-free NaOCl solutions were determined by measuring the absorbance at 292 nm ($\epsilon = 350 \text{ M}^{-1} \text{ cm}^{-1}$) [48]. New solutions of NaOCl were prepared fresh daily prior to each experiment to minimize the spontaneous decomposition of HOCl and to ensure that concentrations were accurate.

2.6. HPLC analysis

HPLC analyses were carried out using an Agilent 1100 series HPLC system equipped with a degasser, quaternary pump, autosampler, and a photodiode array detector (resolution of 2 nm), using either a Phenomenex Luna C₁₈ semipreparative column (5 μm, 100 Å, 10 mm × 300 mm; Methods A + B) or an Alltech Alltima (Grace) C₁₈ semipreparative column (5 μm, 100 Å, 10 mm × 300 mm; Method C) thermostated to 25 °C.

2.7. HPLC analysis of the products of the reaction between Cbl(II) and (H)OCl

a) In the absence of phenol. The product solution of the reaction between Cbl(II) (5.0×10^{-4} M) with (H)OCl (4.5×10^{-4} M) at pH 7.00 under anaerobic conditions (0.100 M phosphate buffer, 25.0 °C, $I = 1.0$ M (NaCF₃SO₃)) was analyzed by HPLC using Method A. b) In the presence of phenol. The product solution of the reaction between Cbl(II) (5.0×10^{-4} M) with (H)OCl (4.5×10^{-4} M) in the presence of phenol (1.25×10^{-2} M) under anaerobic conditions at pH 7.00 (0.100 M phosphate buffer, 25.0 °C, $I = 1.0$ M (NaCF₃SO₃)) was analyzed by HPLC using Method B. c) In the presence of tyrosine. The product solution formed from the reaction between Cbl(II) (5.0×10^{-4} M) with (H)OCl (4.5×10^{-4} M) in the presence of the excess tyrosine (1.25×10^{-2} M) at pH 7.00 (0.100 M phosphate buffer, 25.0 °C, $I = 1.0$ M (NaCF₃SO₃)) was analyzed using Method C. Method A. A mobile phase consisting of acetate buffer (1% v/v CH₃COOH, pH 3.5), A, and CH₃CN, B, was used in the following method: 0–15 min isocratic elution of 94:6 A:B, 15–17 min 94:6 to 30:70 A:B, 17–35 min isocratic elution of 30:70 A:B, 35–37 min 30:70 to 94:6 A:B, 37–40 min isocratic elution of 94:6 A:B. All gradients were linear and a flow rate of 2 ml/min was used. Product peaks were monitored at 350 nm. Method B. A mobile phase consisting of acetate buffer (1% v/v CH₃COOH, pH 3.5), A, and CH₃CN, B, was used as follows: 0–25 min isocratic elution of 50:50 A:B, 25–27 min 50:50 to 30:70 A:B, 27–34 min isocratic elution of 30:70 A:B, 34–36 min 30:70 to 50:50 A:B, 37–40 min isocratic elution of 50:50 A:B. All gradients were linear and a flow rate of 2 ml/min was used. All the standards (phenol, 2-chlorophenol and 4-chlorophenol) were prepared in 0.10 M phosphate buffer, pH 7.00 and diluted as needed. Product peaks were monitored at 280 nm. Method C. A mobile phase consisting of acetate buffer (1% v/v CH₃COOH, pH 3.5), A, and CH₃OH, B, were used in the following method: 0–2 min isocratic elution of 70:30 A:B; 2–5 min, linear gradient to 60:40 A:B; 5–27 min, linear gradient to 55:45 A:B; 27–30 min, linear gradient 20:80 A:B; 30–36 min isocratic elution of 20:80 A:B; 36–38 min, linear gradient 20:80 A:B. The flow rate of 1 ml/min was used. All the standards (tyrosine, 3-hydroxytyrosine) were prepared in 0.10 M phosphate buffer, pH 7.00 and diluted as needed. Product peaks were monitored at 280 nm.

2.8. Ultra high performance liquid chromatography (UHPLC) experiments

UHPLC analyses were carried out using a Dionex UltiMate 3000 rapid separation liquid chromatograph equipped with a degasser, quaternary pump, autosampler, and a photodiode array detector (bandwidth of 2 nm). Analytes were separated on a Thermo Scientific Hypersil GOLD C₁₈ column (1.9 μm, 175 Å, 2.1 mm × 55 mm). The following multistep gradient method with acetate buffer (1% v/v CH₃COOH, pH 3.5), A, and CH₃OH, B, was used to separate constituents: 0–15 min 90:10 to 86:14 A:B, 15–20 min 86:14 to 65:35 A:B, 20–21 min 65:35 to 50:50 A:B, 21–26 min isocratic elution of 50:50 (column rinse), 26–27 min 50:50 to 90:10 A:B, 27–30 min isocratic column conditioning at 90:10 A:B. All gradients were linear and maintained at a flow rate of 0.300 ml/min. Product peaks were monitored at 254 and 350 nm with a reference wavelength of 398 nm. Eluent from the separation was directly infused into the electrospray ionization source of the mass spectrometer, described below.

2.9. High resolution mass spectrometry (HRMS) measurements

High resolution mass spectra of the eluting species were obtained using an Exactive Plus mass spectrometer (Thermo Scientific, Bremen, Germany) equipped with a heated electrospray ionization source (HESI II probe, Thermo Scientific, Bremen, Germany). The source was operated at 3.5 kV with a sheath gas flow rate and gas heater temperature of 25 (manufacturers units) and 310 °C, respectively, to cope with the relatively high liquid flow rates.

Mass spectra were recorded in the positive ionization mode with a scan range of 133–2000 *m/z*, a mass resolving power setting of 140,000, and an automatic gain control (AGC) target value of 1×10^6 ions. To ensure very high mass accuracy (>0.75 mmu), the instrument was calibrated daily and a lock mass of *m/z* 371.10124, due to polysiloxane, was used throughout. These setting resulted in a spectral acquisition rate of ~ 1.9 spectra/s. All UV absorption and mass spectral data were collected and processed with the Xcalibur software (ver. 3.0, Thermo Scientific, San Jose, CA, USA).

3. Results and discussion

The kinetics of the reaction between hypochlorite and the reduced vitamin B₁₂ complex, cob(II)alamin were studied at pH 8.60–12.00 under anaerobic conditions using stopped-flow spectroscopy. The hypochlorite concentration was kept at least 5 times higher than the Cbl(II) concentration, to maintain pseudo-first order conditions. Fig. 2 gives UV–Vis spectra for the reaction between Cbl(II) (4.70×10^{-5} M) and excess OCl[−] (5.00×10^{-3} M) at pH 11.30 (0.100 M phosphate buffer, 25.0 °C, $I = 1.0$ M (NaCF₃SO₃)). Cbl(II) ($\lambda_{\max} = 312, 405, 475$ nm) is converted to hydroxycobalamin (HOcbl; $\lambda_{\max} = 357, 417, 535$ nm) with sharp isobestics observed at 337, 374, 490, and 574 nm, in agreement with literature values for the conversion of Cbl(II) to HOcbl [49]. (Note that HPLC/HRMS experiments show that small amounts of spectrally indistinguishable corrinoids with two or four H atoms fewer than cobalamin are also formed – this will be discussed later.) The inset to Fig. 2 gives the corresponding plot of absorbance at 312 nm versus time. The data fit well to a first-order rate equation, giving $k_{\text{obs}} = (2.61 \pm 0.06) \times 10^2 \text{ s}^{-1}$.

Rate constants for the reaction between Cbl(II) and OCl[−] were also determined at other concentrations at pH 11.30 and the data are summarized in Fig. 3. Data fitted well to a straight line passing through the origin, consistent with a single irreversible reaction. The linear relationship suggests that the reaction is first-order with respect to the concentration of hypochlorite. From the slope, the apparent second-order rate

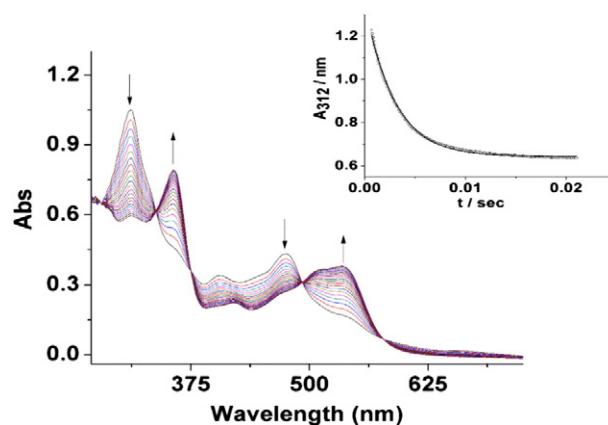


Fig. 2. Plot of absorbance vs wavelength for the reaction of Cbl(II) (4.70×10^{-5} M) with OCl[−] (5.00×10^{-3} M) at pH 11.30 (0.100 M phosphate buffer, $I = 1.0$ M (NaCF₃SO₃), 25.0 °C). Spectra were collected every 2.00 ms for 1.00 s. Inset: The best fit of absorbance data at 312 nm versus time to a first-order rate equation, giving $k_{\text{obs}} = (2.61 \pm 0.06) \times 10^2 \text{ s}^{-1}$.

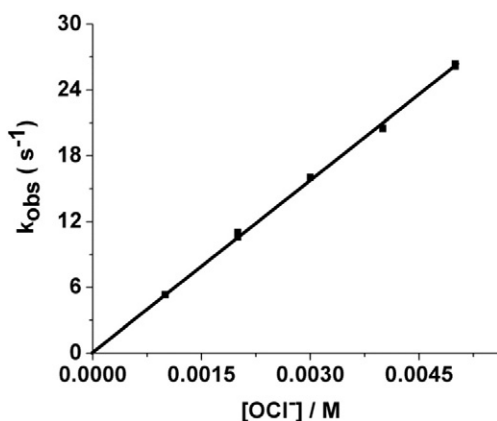


Fig. 3. Plot of k_{obs} versus OCI^- concentration for the reaction between Cbl(II) (5.0×10^{-5} M) and OCI^- at pH 11.30 (0.100 M phosphate buffer, 25.0°C , $I = 1.0$ M (NaCF_3SO_3)). Data were fitted to a line passing through origin, giving $k_{\text{app}} = (5.25 \pm 0.05) \times 10^3 \text{ M}^{-1} \text{ s}^{-1}$.

constant (k_{app}) of the reaction can be calculated and was found to be $(5.25 \pm 0.05) \times 10^3 \text{ M}^{-1} \text{ s}^{-1}$.

The dependence of k_{app} on pH was determined at pH 8.60, 8.80, 9.10, 9.40, 9.74, 10.00, 10.50, and 12.00. Data fitted well to a straight line which passes through the origin at all pH conditions, giving the apparent second-order rate constants, $k_{\text{app}} = (1.38 \pm 0.02) \times 10^6 \text{ M}^{-1} \text{ s}^{-1}$, $(7.45 \pm 0.15) \times 10^5 \text{ M}^{-1} \text{ s}^{-1}$, $(3.97 \pm 0.06) \times 10^5 \text{ M}^{-1} \text{ s}^{-1}$, $(3.36 \pm 0.05) \times 10^5 \text{ M}^{-1} \text{ s}^{-1}$, $(1.36 \pm 0.01) \times 10^5 \text{ M}^{-1} \text{ s}^{-1}$, $(5.95 \pm 0.06) \times 10^4 \text{ M}^{-1} \text{ s}^{-1}$, $(2.12 \pm 0.02) \times 10^4 \text{ M}^{-1} \text{ s}^{-1}$, and $(2.28 \pm 0.02) \times 10^3 \text{ M}^{-1} \text{ s}^{-1}$ at pH 8.60, 8.80, 9.10, 9.40, 9.74, 10.00, 10.50, and 12.00, respectively (Supplemental Information, Figs. S1–S8). The plot in Fig. 4 summarizes the dependence of k_{app} on pH. It is clear from these data that k_{app} increases with decreasing pH. Assuming that both HOCl and OCI^- react with Cbl(II), then,

$$\text{rate} = k_{\text{OCI}^-}[\text{Cbl(II)}][\text{OCI}^-] + k_{\text{HOCl}}[\text{Cbl(II)}][\text{HOCl}] \quad (3)$$

From Eq. (3) it can be shown that

$$k_{\text{app}} = \frac{(k_{\text{HOCl}} \times 10^{-\text{pH}} + k_{\text{OCI}^-} \times K_{\text{a(HOCl)}})}{(K_{\text{a(HOCl)}} + 10^{-\text{pH}})} \quad (4)$$

It was not possible to get a meaningful fit of the experimental data allowing $\text{p}K_{\text{a(HOCl)}}$, k_{HOCl} and k_{OCI^-} to vary (in this case all three values had errors larger than the numbers themselves). The most meaningful fit was instead obtained by fixing $\text{p}K_{\text{a(HOCl)}} = 7.40$ [45] and $k_{\text{OCI}^-} = 2.28 \times 10^3 \text{ M}^{-1} \text{ s}^{-1}$ (the value of k_{app} at pH 12.00), and allowing k_{HOCl} to vary, giving $k_{\text{HOCl}} = (2.60 \pm 0.10) \times 10^7 \text{ M}^{-1} \text{ s}^{-1}$.

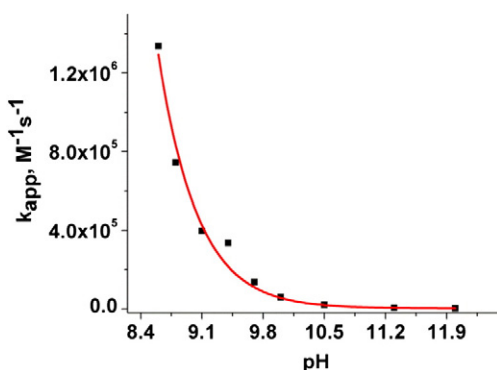


Fig. 4. Plot of k_{app} versus pH. The data were fitted to Eq. (4) in the text fixing $\text{p}K_{\text{a(HOCl)}} = 7.40$ and $k_{\text{OCI}^-} = 2.28 \times 10^3 \text{ M}^{-1} \text{ s}^{-1}$, giving $k_{\text{HOCl}} = (2.60 \pm 0.10) \times 10^7 \text{ M}^{-1} \text{ s}^{-1}$.

The stoichiometry of the reaction between Cbl(II) and OCI^- at pH 11.30 was determined by titration. A solution of Cbl(II) (4.50×10^{-5} M) was left to equilibrate for 10 min with increasing amounts of OCI^- and UV–Vis spectra recorded from 250 to 800 nm. Fig. 5 shows UV–Vis spectra for equilibrated solutions of Cbl(II) with 0–2.25 mol equiv. OCI^- at pH 11.30. The inset to Fig. 5 shows the initial and final spectra for this experiment. The spectrum of the product and the isosbestic wavelengths are once again consistent with formation of HOcbl [49]. From these UV–Vis spectra, a plot of absorbance at 312 nm versus mol equiv. of OCI^- was generated, Fig. 5(b). The absorbance at 312 nm decreases linearly up to 1.0 mol equiv. of OCI^- and is unchanged upon the addition of further OCI^- . This indicates that the stoichiometry of the reaction of Cbl(II) with OCI^- at pH 11.30 is 1:1 Cbl(II): OCI^- . Similar experiments were carried out to determine the stoichiometry at pH 7.00, 9.40, 10.50, and pH 12.00, respectively. The stoichiometry remained 1:1 Cbl(II):(H)OCl for all pH conditions (Figs. S9–S12, Supplemental Information).

To confirm HOcbl formation, the ^1H NMR spectrum of the product solution of the reaction of Cbl(II) with 1.3 equiv. OCI^- was recorded (pD 7.40). Five peaks were observed in the aromatic region of the spectrum at 7.16 (s, B7), 6.73 (s, B2), 6.50 (s, B4), 6.24 (d, R1) and 6.06 (s, C10) ppm, Fig. S13, Supplemental Information, in excellent agreement with chemical shifts reported for HOcbl [44].

With higher concentrations of (H)OCl and at longer reaction times, other reactions were observed after the rapid oxidation of Cbl(II) to HOcbl. Fig. 6 shows UV–Vis spectra for the reaction between Cbl(II) (5.0×10^{-5} M) and excess OCI^- (5.00×10^{-3} M) at pH 11.30 (0.100 M phosphate buffer, 25.0°C , $I = 1.0$ M (NaCF_3SO_3)) over a longer time period (5 min). The first spectrum corresponds to HOcbl. The absorbance of the corrinoid subsequently decreases as a function of time over the entire wavelength range. These spectral changes are consistent with loss of conjugation in the macrocycle, which give rise to intense π to π^* electronic transitions [50]. Electrophilic attack of HOCl at the cobalamin macrocycle may potentially occur, to give cobalamin analogs [14,15,51,52].

To check that the subsequent reactions at longer times had a negligible effect on the second-order rate constants obtained with excess concentrations of HOCl compared to Cbl(II), rate data for the Cbl(II) + HOCl reaction was also obtained with the Cbl(II) concentration in excess. Under these conditions subsequent reactions between HOcbl and HOCl do not occur. Fig. S14 in the Supplemental Information gives a plot of k_{app} versus [Cbl(II)] for the reaction of Cbl(II) (1.00 – $2.50) \times 10^{-4}$ M) with OCI^- (2.00×10^{-5} M) at pH 9.40. The best fit of the data gave $k_{\text{app}} = (3.16 \pm 0.02) \times 10^5 \text{ M}^{-1} \text{ s}^{-1}$, which is in excellent agreement with the value obtained at the same pH condition with the OCI^- concentration in excess ($(3.36 \pm 0.05) \times 10^5 \text{ M}^{-1} \text{ s}^{-1}$). A similar result was also obtained at pH 9.10 ($k_{\text{app}} = (4.01 \pm 0.04) \times 10^5 \text{ M}^{-1} \text{ s}^{-1}$ (Fig. S15, Supplemental Information) versus $(3.97 \pm 0.06) \times 10^5 \text{ M}^{-1} \text{ s}^{-1}$, with [Cbl(II)] or [OCI⁻] in excess, respectively).

Studies of reactions involving (H)OCl are complicated by the presence of chlorine in addition to (H)OCl in the solution, which arises as a consequence of the equilibrium shown in Eq. (2). Both HOCl and Cl_2 are strong oxidants and can oxidize Cbl(II). The redox potentials are $2\text{HOCl}, 2\text{H}^+/\text{Cl}_2, 2\text{H}_2\text{O} = 1.61$ V versus NHE [53], $\text{Cl}_2/\text{Cl}_2^- = 0.43$ V versus NHE [22] and $\text{H}_2\text{OCbl}^+/\text{Cbl(II)} = 0.20$ V versus NHE [54]. Indeed, it has been suggested that Cl_2 , not HOCl, is the cytotoxic species generated by the heme enzyme myeloperoxidase [8,28], and others have shown that Cl_2 can react faster with transition metal complexes compared with HOCl under acidic conditions [24]. Experiments were therefore carried out to confirm that HOCl, not Cl_2 , oxidizes Cbl(II) to HOcbl. If indeed Cl_2 is the oxidant, more Cl_2 will be generated in solution in the presence of Cl^- , Eq. (2), and the addition of Cl^- to the solution will therefore increase the observed rate constant for the reaction. To ensure that the solution did not contain trace amounts of Cl^- for these experiments, strictly chloride-free NaOCl was prepared using a literature

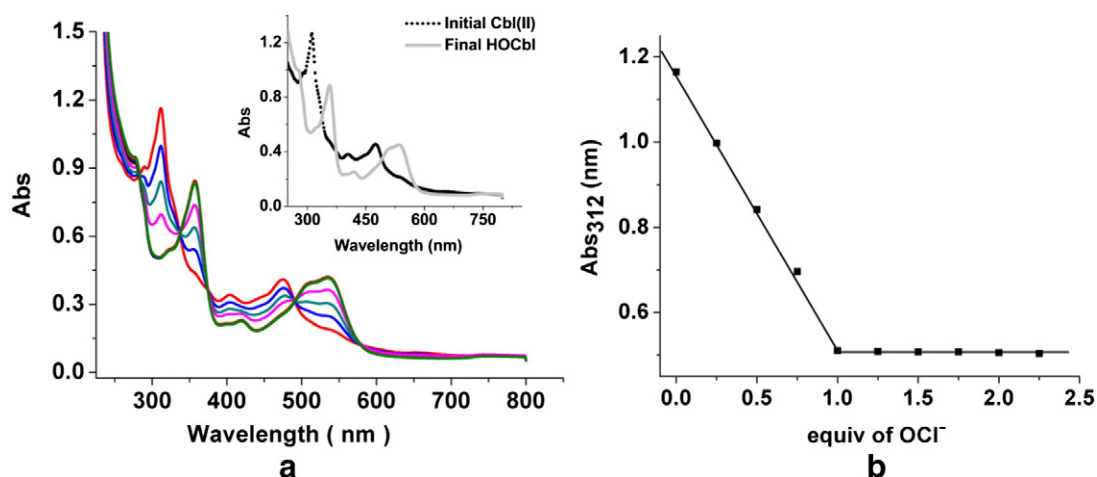
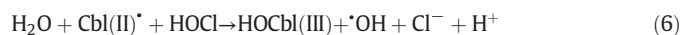


Fig. 5. (a) UV-Vis spectra for equilibrated solutions of Cbl(II) with 0–2.25 mol equivalents of OCl^- at pH 11.30 (0.100 M phosphate, $I = 1.0$ M (NaCF_3SO_3), 25.0°C). Inset: initial and final spectra. (b) Plot of absorbance at 312 nm versus mole equiv. OCl^- for the data shown in (a). Spectra for ≥ 1 mol equiv. OCl^- are practically indistinguishable from each other.

procedure (see [Experimental section](#)) [8] and the observed rate constant for the reaction between Cbl(II) and OCl^- was determined in the presence of varying concentrations of Cl^- . Reactions were carried out between Cbl(II) (5.0×10^{-5} M) with excess chloride-free OCl^- (1.0×10^{-3} M) at pH 10.00 (0.10 M phosphate buffer, 25.0°C , $I = 1.00$ M (NaCF_3SO_3)). Figs. S16–18 in the Supplemental Information show plots of absorbance at 312 nm versus time for the reaction between Cbl(II) (5.0×10^{-5} M) and chloride-free OCl^- (1.0×10^{-3} M) in the presence and absence of added chloride (1.0×10^{-3} M or 5.0×10^{-3} M), giving $k_{\text{obs}} = 41.8 \pm 0.1$, 41.4 ± 0.1 and 41.5 ± 0.1 s^{-1} , respectively. These values are comparable with k_{obs} reported for the reaction between Cbl(II) (5.0×10^{-5} M) and OCl^- (1.0×10^{-3} M) at pH 10.00 ($k_{\text{obs}} = 45.1 \pm 0.1$ s^{-1}). These results are consistent with HOCl, not Cl_2 , being the oxidant.

Others have reported that $1e^-$ oxidation of Fe^{2+} to Fe^{3+} by HOCl generates chlorine radicals [26,55] or hydroxyl radicals [1,55]. Both of these pathways are consistent with the 1:1 Cbl(II):HOCl stoichiometry results; Eqs. (5) and (6).



HPLC was used to further probe the initial products of the reaction between Cbl(II) and (H)OCl. Fig. S19(a) in the Supplemental Information shows the HPLC chromatogram of the product solution formed

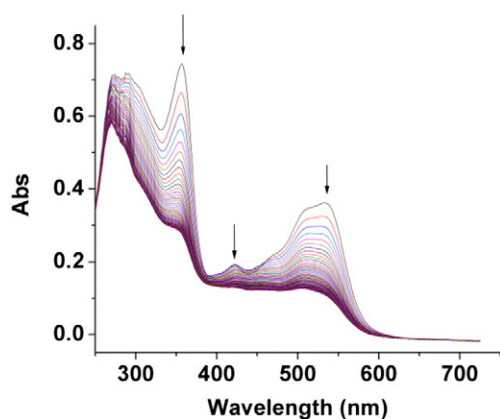


Fig. 6. Plot of absorbance vs wavelength for the reaction of Cbl(II) (5.00×10^{-5} M) with OCl^- (5.00×10^{-3} M) at pH 11.30 (0.100 M phosphate buffer, $I = 1.0$ M (NaCF_3SO_3), 25.0°C). Spectra were collected every 3.00 s for 5.00 min.

from the reaction between Cbl(II) (5.0×10^{-4} M) with 0.90 mol equiv. (H)OCl (pH 7.00, 0.10 M phosphate buffer, 25.0°C , $I = 1.0$ M (NaCF_3SO_3)) using an isocratic method (Method A). The major peak at 9.2 min can be attributed to H_2OCbl^+ . The minor peaks in the ~5–8 min region are not observed for an authentic sample of H_2OCbl^+ (Fig. S20, Supplemental Information), and therefore most likely arise from modified corrinoid species formed when the radical produced upon $1e^-$ reduction of HOCl by Cbl(II) (either $\cdot\text{OH}$ or Cl^{\cdot}) reacts with the corrin macrocycle (see below). The small bump at ~23 min observed during washing of the column was also observed for authentic H_2OCbl^+ when an isocratic elution method was used (see Fig. S20 in the Supplemental Information).

To probe whether Cl^{\cdot} and/or $\cdot\text{OH}$ production directly or indirectly leads to the complexes which elute in the ~5–8 min region of the chromatogram, the HPLC chromatogram of the product solution of the reaction between Cbl(II) (5.0×10^{-5} M) and (H)OCl (0.90 mol equiv.) in the presence of a large excess of the efficient radical scavenger phenol [$56\text{--}58$] (1.25×10^{-2} M) was obtained, Fig. S21. The significant reduction in the intensity of peaks in the ~5–8 min region compared with the spectrum shown in Fig. S19(a) provides indirect evidence for these complexes arising from a subsequent reaction of a radical intermediate with the corrin macrocycle. Using this HPLC elution method, chlorinated phenols elute with almost the same retention times as phenol itself. A new HPLC method (Method B) was therefore developed using authentic samples of all compounds, to separate phenol from the potential chlorinated phenols 2-chlorophenol and 4-chlorophenol (see Fig. S22, Supplemental Information). However HPLC experiments could not unequivocally establish whether Cl^{\cdot} is a reaction intermediate, since (H)OCl directly chlorinates phenol (see Fig. S23, Supplemental Information) [59,60].

A significantly more sensitive method is Ultra High Performance Liquid Chromatography combined with High Resolution Mass Spectrometry (UHPLC/HRMS; mass accuracies better than 0.0008 Da). The product solution of the reaction of Cbl(II) (5.0×10^{-5} M) with 0.9 mol equiv. OCl^- (pH 7.00, 0.050 M KH_2PO_4 , RT) was therefore subsequently analyzed by UHPLC/HRMS, Fig. S25(a) in the Supplemental Information. A UHPLC/HRMS chromatogram was also obtained for a Cbl(III) solution, prepared by the oxidation of Cbl(II) (5.0×10^{-5} M) by air (pH 7.00, 0.050 M KH_2PO_4 , RT) for comparison purposes, Fig. S25(b). Peak assignments for both the product solution and the control are given in Table S1 and S2, respectively, in the Supplemental Information. Assignments for the peaks that were significantly more intense in the former sample compared with the control are given in Table 1, and can be attributed to corrinoid species with two (Cbl-2H) or four (Cbl-4H) hydrogen atoms fewer than cobalamin. A peak was also observed in the

Table 1
Mass assignments for ion signals (m/z) which were significantly more intense in the product solution of the reaction between Cbl(II) (5.0×10^{-5} M) and 0.9 mol equiv. OCl⁻ compared to the solution of Cbl(II) oxidized to Cbl(III) by air (pH 7.00, 0.050 M KH₂PO₄, RT).

Retention time (min)	Elemental composition	Shorthand notation	Monoisotopic mass, m/z (Calc)	Monoisotopic mass, m/z (actual)	Signal intensity
1.52	C ₆₂ H ₉₁ O ₁₆ N ₁₃ CoP	[(H ₂ OCbl-2H) + H ₂ O + H] ²⁺	681.7883	681.7886	2.3×10^5
1.62	C ₆₂ H ₈₉ O ₁₅ N ₁₃ CoP	[(H ₂ OCbl-2H) + H] ²⁺	672.7830	672.7833	8.8×10^5
1.87	C ₆₂ H ₈₉ O ₁₅ N ₁₃ CoP	[(H ₂ OCbl-2H) + H] ²⁺	672.7830	672.7833	9.3×10^5
2.58	C ₆₂ H ₈₇ O ₁₅ N ₁₃ CoP	[(H ₂ OCbl-4H) + H] ²⁺	671.7752	671.7754	1.2×10^8
2.81	C ₆₂ H ₈₉ O ₁₅ N ₁₃ CoP	[(H ₂ OCbl-2H) + H] ²⁺	672.7830	672.7836	1.4×10^5
3.00	C ₆₂ H ₈₉ O ₁₅ N ₁₃ CoP	[(H ₂ OCbl-2H) + H] ²⁺	672.7830	672.7830	1.8×10^6
4.60	C ₆₂ H ₈₈ O ₁₄ N ₁₃ CoPCI	[(Cbl + Cl-H) + H] ²⁺	681.7662	681.7662	2.3×10^5

product solution only which can be assigned to a corrinoid species in which a H atom is replaced by a Cl atom (Cbl + Cl-H). There is excellent agreement between the calculated and experimentally observed isotopic pattern for this latter peak, Fig. S26, Supplemental Information. Both the Cl• and HO• radicals are well-known to abstract H atoms [61, 62]. H atoms of the cobalamin moiety susceptible to abstraction include the C3, C8, C13, C18 and C19 carbons of the corrin ring [63]. It was recently proposed that subsequent to H atom abstraction from one of these C centers of Cbl(III) by the carbonate radical, a H atom on an adjacent C atom is abstracted to yield a species with two fewer H atoms (H₂OCbl-2H) compared with the parent macrocycle [63]. The H₂OCbl-2H product reacts further via a similar mechanism to generate a H₂OCbl-4H species [63].

Interestingly, for hexacyanoferrate(II) a 1:2 [Fe(CN)₆]²⁺:HOCl stoichiometry was observed, and it was proposed that Cl• produced from the oxidation of [Fe(CN)₆]²⁺ to [Fe(CN)₆]³⁺ by HOCl also oxidizes [Fe(CN)₆]²⁺ to [Fe(CN)₆]³⁺ [26]. Our 1:1 Cbl(II):HOCl stoichiometry is, however, not consistent with oxidation of Cbl(II) by Cl•. Cl• could potentially also react with solvent H₂O, although this reaction is not particularly rapid ($k_{\text{obs}} = 2 \times 10^5 \text{ s}^{-1}$) [64].

HPLC experiments were also carried out to further probe if •OH is produced as a product of the oxidation of Cbl(II) by HOCl using the efficient •OH scavenger, tyrosine (Tyr) [65]. The product solution of the reaction between Cbl(II) (5.0×10^{-5} M) and (H)OCl (0.90 mol equiv.) in the presence of a large excess of tyrosine (1.25×10^{-2} M) was analyzed using HPLC (Method C; see Fig. S27, Supplemental information). Tyrosine and 3-hydroxytyrosine standards were run individually to determine their retention times (see Fig. S28 (a–b), Supplemental Information). However 3-hydroxytyrosine was not observed in the chromatogram, indicating that •OH generation from the oxidation of Cbl(II) by HOCl is minimal.

All classes of biomolecules are damaged by HOCl, including lipids, carbohydrates, nucleic acids and proteins such as lactoperoxidase, horseradish peroxidase and myoglobin [1,7–17]. Vitamin B₁₂ and its derivatives (cob(III)alamins) are reduced to Cbl(II) upon entering cells [31], and with supplementation a substantial proportion (up to ~50%) of cytosolic and mitochondrial Cbl exists in its free (non-protein bound) form [32–36]. Cbls show potential as efficient intracellular scavengers of other ROS/RNS including superoxide [37,38], and it is likely that Cbl(II) is the active Cbl form. Given that the rate constant for the reaction of Cbl(II) with HOCl is so rapid, HOCl should preferentially react with Cbl(II) rather than reacting with other biomolecules. To probe this further, the ability of Cbl(II) to prevent HOCl-induced damage of the protein bovine serum albumin (BSA) was investigated. Others have reported that the HOCl-induced fragmentation of albumin primarily arises from chlorination of the amide N atoms leading to peptide bond cleavage [1,12]. Wells 1–4 of Fig. 7 show a reducing SDS-PAGE gel of the product solution obtained upon exposing BSA (0.27 μM) to increasing concentrations of HOCl (0, 50, 100 and 250 μM; pH 7.00, 0.10 M phosphate buffer, RT). BSA is completely destroyed by HOCl (250 μM). However exposing BSA to HOCl (250 μM) in the presence of Cbl(II) (1.0, 2.0, 10 and 20 mol equiv., wells 5–8) increasingly protects the protein from HOCl-induced damage. These data suggest that Cbl(II) is an extremely good scavenger of HOCl. However further studies are required to establish if indeed reactions of this type are biologically relevant.

Finally, others have reported kinetic studies on the reaction between cyanocobalamin and HOCl (pH 7.00) [3]. CNCl is formed and LC/MS evidence for a CNCl complex minus a H atom and a chlorinated cyanocobalamin species was presented. It is proposed that HOCl substitutes the α-dimethylbenzimidazole based on UV-vis spectral changes, followed by nucleotide and corrin ring destruction. Although two observed rate

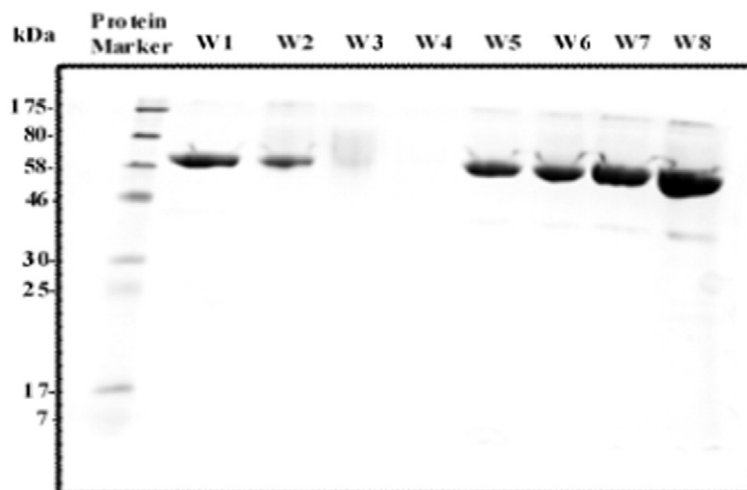


Fig. 7. Reducing SDS-PAGE gel of BSA (0.27 μM) treated with (H)OCl in the absence (Wells 1–4) and presence (Wells 5–8) of Cbl(II) under anaerobic conditions. Well 1 (W1): 0 M (H)OCl; W2: 50 μM (H)OCl; W3: 100 μM (H)OCl; W4: 250 μM (H)OCl; W5: 250 μM (H)OCl + 250 μM Cbl(II); W6: 250 μM (H)OCl + 500 μM Cbl(II); W7: 250 μM (H)OCl + 2.50 mM Cbl(II); W8: 250 μM (H)OCl + 5.00 mM Cbl(II). The protein band at ~66 kDa corresponds to BSA.

constants of almost equal magnitudes are reported, the assignment of them to specific steps is somewhat speculative and it is possible that they are in fact mixed values, given the reactivity of HOCl and a plot of observed rate constant versus (H)OCl increases exponentially.

4. Conclusions

Kinetic and mechanistic studies on the reaction between Cbl(II) and (H)OCl have been carried out using UV–Vis spectroscopy and stopped-flow spectroscopy. The apparent rate constant, k_{app} , increases as the pH decreases, and rate constants for the reaction of HOCl and OCl⁻ with Cbl(II) were $2.6 \times 10^7 \text{ M}^{-1} \text{ s}^{-1}$ and $2.3 \times 10^3 \text{ M}^{-1} \text{ s}^{-1}$, respectively. The observed second-order rate constant for the reaction at pH 7.00 is large ($1.8 \times 10^7 \text{ M}^{-1} \text{ s}^{-1}$), and at pH 7.00 and 5 mM HOCl, the half-life of the reaction is $\sim 8 \times 10^{-3}$ ms. UHPLC/HRMS studies of the products of the reaction between Cbl(II) and 0.9 mol equiv. (H)OCl provide evidence for formation of multiple modified corrinoid species including (Cbl-2H), (Cbl-4H) and a complex in which a H atom of the cobalamin has been substituted with a Cl atom. No evidence for a •OH intermediate was found using a tyrosine scavenger. SDS-PAGE experiments show that rapid scavenging of HOCl by Cbl(II) prevents HOCl-induced damage to bovine serum albumin.

Appendix A. Supplementary data

Additional kinetic data, stoichiometry data, ¹H NMR data and HPLC chromatograms; Figs. S1–S25. This material is available alongside the electronic version of the article in Elsevier Web products, including ScienceDirect: <http://www.sciencedirect.com>. Supplementary data associated with this article can be found in the online version, at <http://dx.doi.org/10.1016/j.jinorgbio.2016.07.009>.

References

- [1] O.M. Panasenko, I.V. Gorudko, A.V. Sokolov, *Biochemistry (Mosc)* 78 (2013) 1466–1489.
- [2] G. Bauer, *Anticancer Res.* 33 (2013) 3589–3602.
- [3] H.M. Abu-Soud, D. Maitra, J. Byun, C.E.A. Souza, J. Banerjee, G.M. Saed, M.P. Diamond, P.R. Andreana, S. Pennathur, *Free Radic. Biol. Med.* 52 (2012) 616–625.
- [4] S.J. Weiss, *N. Engl. J. Med.* 320 (1989) 365–376.
- [5] A. Vivekanadan-Giri, J.H. Wang, J. Byun, S. Pennathur, *Rev. Endocr. Metab. Disord.* 9 (2008) 275–287.
- [6] Y.W. Yap, M. Whiteman, N.S. Cheung, *Cell. Signal.* 19 (2007) 219–228.
- [7] I.V. Gorudko, D.V. Grigorieva, E.V. Shamova, V.A. Kostevich, A.V. Sokolov, E.V. Mikhailchik, S.N. Cherenkevich, J. Arnhold, O.M. Panasenko, *Free Radic. Biol. Med.* 68 (2014) 326–334.
- [8] J.P. Henderson, J. Byun, J.W. Heinecke, *J. Biol. Chem.* 274 (1999) 33440–33448.
- [9] J.K. Hurst, W.C. Barrette, B.R. Michel, H. Rosen, *Eur. J. Biochem.* 202 (1991) 1275–1282.
- [10] J.J.I. Kang, J.W. Neidigh, *Chem. Res. Toxicol.* 21 (2008) 1028–1038.
- [11] A. Robaszekiewicz, G. Bartosz, A.R. Pitt, A. Thakker, R.A. Armstrong, C.M. Spickett, M. Soszynski, *Arch. Biochem. Biophys.* 548 (2014) 1–10.
- [12] J.D. Sivey, S.C. Howell, D.J. Bean, D.L. McCurry, W.A. Mitch, C.J. Wilson, *Biochemistry* 52 (2013) 1260–1271.
- [13] C.E.A. Souza, D. Maitra, G.M. Saed, M.P. Diamond, A.A. Moura, S. Pennathur, H.M. Abu-Soud, *PLoS One* 6 (2011), e27641.
- [14] J.M. Albrich, C.A. McCarthy, J.K. Hurst, *Proc. Natl. Acad. Sci.* 78 (1981) 210–214.
- [15] S. Ozaki, C. Dairaku, Y. Kuradomi, J. Inoue, *Chem. Lett.* 37 (2008) 666–667.
- [16] L. Gebicka, E. Banasiak, *Toxicol. in Vitro* 26 (2012) 924–929.
- [17] J.S. Møller, L. Skibsted, *J. Biol. Inorg. Chem.* 19 (2014) 805–812.
- [18] Q. Xu, K.A. Lee, S. Lee, K.M. Lee, W.J. Lee, J. Yoon, *J. Am. Chem. Soc.* 135 (2013) 9944–9949.
- [19] R. Zhang, Z. Ye, B. Song, Z. Dai, X. An, J. Yuan, *Inorg. Chem.* 52 (2013) 10325–10331.
- [20] G.H. Ayres, M.H. Booth, *J. Am. Chem. Soc.* 77 (1955) 825–827.
- [21] R.W. Lee, P.C. Nakagaki, T.C. Bruce, *J. Am. Chem. Soc.* 111 (1989) 1368–1372.
- [22] M.W. Beach, D.W. Margerum, *Inorg. Chem.* 29 (1990) 1225–1232.
- [23] R.A. Silverman, G. Gordon, *Inorg. Chem.* 15 (1976) 35–39.
- [24] R.D. Cornelius, G. Gordon, *Inorg. Chem.* 15 (1976) 1002–1006.
- [25] L. Drougge, L.I. Elding, *Inorg. Chem.* 24 (1985) 2292–2297.
- [26] L. Hin-Fat, *J. Chem. Soc. Dalton Trans.* 2 (1988) 273–275.
- [27] H. Jiang, L. Rao, Z. Zhang, D. Rai, *Inorg. Chim. Acta* 359 (2006) 3237–3242.
- [28] S.L. Hazen, F.F. Hsu, D.M. Mueller, J.R. Crowley, J.W. Heinecke, *J. Clin. Invest.* 98 (1996) 1283–1289.
- [29] R. Banerjee, *Chemistry and Biochemistry of B₁₂*, Wiley, New York, 1999 1–300.
- [30] L. Randaccio, S. Geremia, N. Demitri, J. Wuerges, *Molecules* 15 (2010) 3228–3259.
- [31] Z. Li, C. Gherasim, N.A. Lesniak, R. Banerjee, *J. Biol. Chem.* 289 (2014) 16487–16497.
- [32] N. Dan, D.F. Cutler, *J. Biol. Chem.* 269 (1994) 18849–18855.
- [33] W.A. Fenton, L.M. Ambani, L.E. Rosenberg, *J. Biol. Chem.* 251 (1976) 6616–6623.
- [34] C.A. Hall, P.D. Green-Colligan, J.A. Begley, *J. Cell. Physiol.* 124 (1985) 507–515.
- [35] J.F. Kolhouse, R.H. Allen, *Proc. Natl. Acad. Sci. U. S. A.* 74 (1977) 921–925.
- [36] E.V. Quadros, D.W. Jacobsen, *Biochim. Biophys. Acta* 1244 (1995) 395–403.
- [37] E.S. Moreira, N.E. Brasch, J. Yun, *Free Radic. Biol. Med.* 51 (2011) 876–883.
- [38] E.S. Moreira, J. Yun, C.S. Birch, J.H.H. Williams, A. McCaddon, N.E. Brasch, *J. Am. Chem. Soc.* 131 (2009) 15078–15079.
- [39] C.S. Birch, N.E. Brasch, A. McCaddon, J.H.H. Williams, *Free Radic. Biol. Med.* 47 (2009) 184–188.
- [40] T.F. Hardlei, E. Nexo, *Clin. Chem.* 55 (2009) 1002–1010.
- [41] A. McCaddon, P. Hudson, L. Abrahamsson, H. Olofsson, B. Regland, *Dement. Geriatr. Cogn. Disord.* 12 (2001) 133–137.
- [42] R. Carmel, D.S. Karnaze, J.M. Weiner, *J. Lab. Clin. Med.* 111 (1988) 57–62.
- [43] H. Kondo, J.F. Kolhouse, R.H. Allen, *Proc. Natl. Acad. Sci. U. S. A.* 77 (1980) 817–821.
- [44] N.E. Brasch, R.G. Finke, *J. Inorg. Biochem.* 73 (1999) 215–219.
- [45] L.C. Adam, I. Fabian, K. Suzuki, G. Gordon, *Inorg. Chem.* 31 (1992) 3534–3541.
- [46] H.A. Barker, R.D. Smyth, H. Weissbach, J.I. Toohey, J.N. Ladd, B.E. Volcani, *J. Biol. Chem.* 235 (1960) 480–488.
- [47] D.W. Johnson, D.W. Margerum, *Inorg. Chem.* 30 (1991) 4845–4851.
- [48] P. Nagy, C.C. Winterbourn, *Chem. Res. Toxicol.* 23 (2010) 1541–1543.
- [49] R. Mukherjee, N.E. Brasch, *Chem. Eur. J.* 17 (2011) 11805–11812.
- [50] J.M. Pratt, *Inorganic Chemistry of Vitamin B₁₂*, Academic Press, London, New York, 1972 100–104.
- [51] J.D. Sivey, A.L. Roberts, *Environ. Sci. Technol.* 46 (2012) 2141–2147.
- [52] C.M. Spickett, A. Jerlich, O.M. Panasenko, J. Arnhold, A.R. Pitt, T. Stelmaszynska, R.J. Schaur, *Acta Biochim. Pol.* 47 (2000) 889–899.
- [53] A.S. Dutton, J.M. Fukuto, K.N. Houk, *Inorg. Chem.* 44 (2005) 4024–4028.
- [54] D. Lexa, J.M. Saveant, *Acc. Chem. Res.* 16 (1983) 235–243.
- [55] L.K. Folkes, L.P. Candeias, P. Wardman, *Arch. Biochem. Biophys.* 323 (1995) 120–126.
- [56] R. Buchacek, G. Gordon, *Inorg. Chem.* 11 (1972) 2154–2160.
- [57] M.G. Ondrus, G. Gordon, *Inorg. Chem.* 11 (1972) 985–989.
- [58] J. Bonin, I. Janik, D. Janik, D.M. Bartels, *J. Phys. Chem. A* 111 (2007) 1869–1878.
- [59] G.F. Lee, J.C. Morris, *Int. J. Air Water Pollut.* 6 (1962) 419–431.
- [60] H. Gallard, U. von Gunten, *Environ. Sci. Technol.* 36 (2002) 884–890.
- [61] L. Sheps, A.C. Crowther, C.G. Elles, F.F. Crim, *J. Phys. Chem. A* 109 (2005) 4296–4302.
- [62] S. Mitroka, S. Zimmeck, D. Troya, J.M. Tanko, *J. Am. Chem. Soc.* 132 (2010) 2907–2913.
- [63] R.S. Dassanayake, J.T. Shelley, D.E. Cabelli, N.E. Brasch, *Chem – Eur. J.* 21 (2015) 6409–6419.
- [64] G.V. Buxton, M. Bydder, G. Arthur Salmon, *J. Chem. Soc. Faraday Trans.* 94 (1998) 653–657.
- [65] H. Subedi, N.E. Brasch, *Inorg. Chem.* 52 (2013) 11608–11617.